ELSEVIER

Biophysical Chemistry 116 (2005) 167 – 173

Biophysical Chemistry

http://www.elsevier.com/locate/biophyschem

The *nop* gene from *Phanerochaete chrysosporium* encodes a peroxidase with novel structural features

Luis F. Larrondo[a], Angel Gonzalez[b], Tomas Perez-Acle[b], Dan Cullen[c], Rafael Vicuña[a,*]

[a]*Departamento de Genética Molecular y Microbiología, Facultad de Ciencias Biológicas, Pontificia, Universidad Católica de Chile, Santiago, Chile and Instituto Milenio de Biología Fundamental y Aplicada, Alameda 340, Santiago, Chile*

[b]*Centro de Genómica y Bioinformática, Pontificia, Universidad Católica de Chile, Alameda 340, Santiago, Chile*

[c]*USDA Forest Products Laboratory, 1 Gifford Pinchot Dr. Madison, Wisconsin 53705, USA*

Received 24 January 2005; accepted 5 March 2005
Available online 4 May 2005

Abstract

Inspection of the genome of the ligninolytic basidiomycete *Phanerochaete chrysosporium* revealed an unusual peroxidase-like sequence. The corresponding full length cDNA was sequenced and an archetypal secretion signal predicted. The deduced mature protein (NoP, novel peroxidase) contains 295 aa residues and is therefore considerably shorter than other Class II (fungal) peroxidases, such as lignin peroxidases and manganese peroxidases. Comparative modeling of NoP was conducted using the crystal structures of *Coprinus cinereus* and *Arthromyces ramosus* peroxidases as templates. The model was validated by molecular dynamics and showed several novel structural features. In particular, NoP has only three disulfide bridges and tryptophan replaces the distal phenylalanine within the heme pocket.
© 2005 Elsevier B.V. All rights reserved.

Keywords: Oxidoreductase; Peroxidase; *Phanerochaete chrysosporium*; Modeling; Molecular dynamics

1. Introduction

Peroxidases are heme-containing proteins catalyzing the oxidation of a variety of substrates using hydrogen peroxide as electron acceptor. Their reaction scheme has been well characterized [1]. First, hydrogen peroxide accepts two electrons from the heme group giving rise to an oxidized form of the enzyme termed compound I. Then, the enzyme undergoes two successive one-electron reductions by its substrate, resulting in formation of compound II and resting enzyme, respectively. Peroxidases can be classified into two large families: one comprising peroxidases from bacteria, fungi and plants, and a second including those from animals [2]. The former family has three major classes [3]: intracellular peroxidases (Class I), secretory fungal peroxidases (Class II) and secretory plant peroxidases (Class III).

Class II enzymes produced by white rot basidiomycetes play a major role in degrading lignin, the second most abundant deposit of carbon. These fungi secrete various types of peroxidases to the extracellular medium [4]. Lignin peroxidase (LiP), which is characterized by its high redox potential and low pH optimum, possesses the unique ability to attack non-phenolic residues generating cation radicals that decay to smaller compounds. Another class II ligninolytic enzyme is manganese peroxidase (MnP), which oxidizes Mn^{2+} to Mn^{3+}. The latter, chelated by organic acids, oxidizes phenolic compounds. Some fungi also produce versatile peroxidase (VP), which oxidizes both Mn^{2+} and non-phenolic compounds. These three peroxidases are monomeric glycoproteins containing either four (LiP and VP) or five (MnP) conserved disulfide bridges and two calcium binding sites [4].

Abbreviations: LiP, lignin peroxidase; MnP, manganese-dependent peroxidase; MD, molecular dynamics; RMSD, root-mean-square deviation; VP or VS, versatile peroxidase; CiP, peroxidase from *Coprinus cinereus*; ARP, peroxidase from *Arthromyces ramosus*.

* Corresponding author. Departamento de Genética Molecular y Microbiología, Facultad de Ciencias Biológicas, Pontificia Universidad Católica de Chile, Casilla 114-D, Santiago, Chile. Tel.: +56 2 6862663; fax: +56 2 2225515.

E-mail address: rvicuna@bio.puc.cl (R. Vicuña).

0301-4622/$ - see front matter © 2005 Elsevier B.V. All rights reserved.
doi:10.1016/j.bpc.2005.03.006

Phanerochaete chrysosporium is the most thoroughly studied white rot fungus [5]. Its recently sequenced genome confirmed the presence of ten genes encoding LiP and five genes encoding MnP, two of which were previously unknown [6]. Inspection of this genome confirmed that *P. chrysosporium* does not produce a phenoloxidase called laccase [7,8], thus solving an old controversy in the field of ligninolysis [9–11].

Further genome analysis led us to the discovery of an actively transcribed gene encoding a novel peroxidase, whose characteristics are presented below.

2. Experimental

2.1. Fungal strains and culture conditions

P. chrysosporium homokaryotic strain RP-78 [12], dikaryotic strains BKM-F-1767 and ME446 were obtained from the Center for Mycology Research, Forest Products Laboratory, Madison, Wisconsin. The fungus was grown for 6 days in defined media containing wood-derived crystalline cellulose (Avicel) [13].

2.2. cDNA cloning and analysis

RNA was extracted from frozen mycelia as described [14]. Poly(A)-RNA was isolated using magnetic capture with oligo dT25 Dynabeads (Dynal, Great Neck, N.Y.). cDNAs were obtained by RT-PCR amplification of the purified poly(A)-RNA as described (Wymelenberg et al. [13]), using as primers the oligonucleotides 5′-CGCTC-TTGCTCTCGACCACC-3′ (forward) and 5′-ACAGTTAT-GAGAGCATGAAT-3′ (reverse). The RT-PCR products were cloned into pGEM-T easy vector (Promega, Madison, WI) and transformed into *E. coli* DH5α cells (Stratagene, La Jolla, CA) following standard procedures [15]. Nucleotide sequences were determined with the ABI Prism Big Dye Terminator Cycle Sequencing kit (Perkin–Elmer Applied Biosystems, Foster City, CA) on ABI automated sequencers. Nucleotide and amino acid sequence similarity searches used BLAST [16] available at the National Center for Biotechnology Information databases. Nucleotide and amino acid sequences were analyzed with DNASTAR software (DNASTAR, Madison, WI). Genomic nucleotide sequence of *nop* is available at http://www.genome.jgi-psf.org/whiterot1/whiterot1.home.html.

2.3. Cladistic analysis

Multiple alignment and phylogenetic analysis were performed over 40 peroxidase sequences with Clustal X v 1.83 using a BLOSUM62 substitution matrix [17]. Gap opening and gap extension penalties were set to 8.0 of 0.1, respectively. Positions of conserved aa residues in the resultant alignment were consistent with the multiple sequences alignment of fungal peroxidases reported by Martinez [4]. The UPGMA distance method was used to produce a phylogenetic tree from the above alignment [18], using MEGA 3.0 program [19]. Standard error was estimated by the bootstrap method, with 1000 replicates, and the Poisson correction distance was employed as criterion for amino acid substitution [20].

2.4. Protein modeling

Modeller-6 [21] within InsightII (Accelrys Inc., San Diego, CA) was employed to develop a comparative model of NoP, using Class II peroxidases from *Coprinus cinereus* and *Arthromyces ramosus* as templates (Brookhaven Protein Data Bank, PDB codes: 1LYK, 1LY8, and 1CK6). Thirty models were generated and ranked by analysis of their stereochemistry using Modeller and Procheck [22]. Ordered results were additionally ranked using the score calculated by the Verify-3D program based on the inverse folding approach [23,24]. From these criteria, the top resulting model was selected as starting point for simulation steps.

2.5. Molecular dynamics (MD) simulation

The protoporphyrin IX containing Fe^{3+} (heme group) was placed in the NoP heme pocket and two Ca^{2+} ions were positioned at metal binding sites, according to X-ray structures of the templates [25,26]. To maintain the distal Ca^{2+} coordination geometry [27,28], two crystallographic calcium sustaining water molecules were added by template superimposition. MD simulations were run using Discover within InsightII with the extensible systematic force field (ESFF; Accelrys Inc., San Diego, CA). The system was energy minimized using a combination of steepest descents and conjugate gradients algorithms until reaching a plateau of 0.01 Kcal mol^{-1} $Å^{-1}$. The MD equilibrium stage was carried out at 300 K for 200 ps, using a quadratic force constraint of 20 Kcal mol^{-1} $Å^{-2}$ over Ca^{2+} and backbone atoms. Finally, a 2 ns, 300 K collect stage was run over the entire system without any constraint. For non-bonded calculations, the cell multipole method with a dielectric constant of 80 was used. Trajectories were recorded every picosecond interval and analyzed using DeCypher within InsightII (Accelrys Inc., San Diego, CA). The final structure was evaluated for quality with Procheck [22].

3. Results and discussion

3.1. Characterization of the nop gene

Analysis of the *P. chrysosporium* genome revealed a putative peroxidase encoding sequence located in scaffold 91 and designated gene model pc.91.32.1 [6]. Close inspection of the model suggested errors. A new model

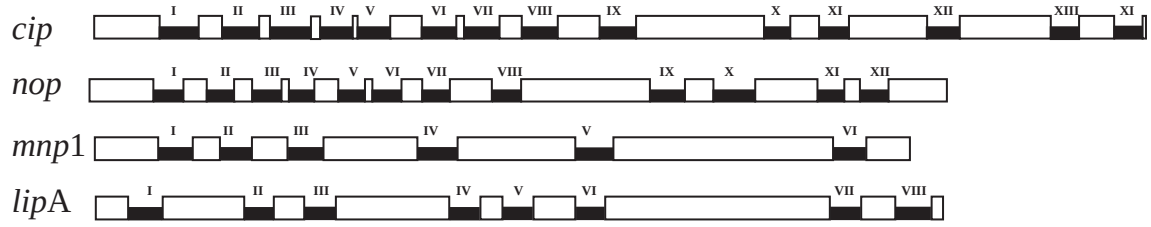

Fig. 1. Intron–exon structure of *nop*, *mnp1*, *lipA* and *cip* genes (GenBank accession numbers AY727765, M60672, M27401 and X70789, respectively). Exons are represented as open boxes and introns as solid black lines.

was constructed and subsequently confirmed by cDNA cloning. Comparison of the *nop* gene with its corresponding cDNA (GenBank accession no. AY727765) revealed twelve introns, all following the GT-AG rule. The intron–exon composition of *nop* has no resemblance with those of *mnp* and *lip* genes from *P. chrysosporium*, which possess 6–7 and 8–9 introns, respectively [4]. However, *nop* harbors a remarkable correspondence with the *cip* gene (Fig. 1). The latter, encoding a peroxidase in the fungus *C. cinereus* [29] contains fourteen introns, ten of which coincide with intron positions in the *nop* gene.

While non-ligninolytic fungi such as *C. cinereus* do not exhibit multiplicity of peroxidase genes, in *P. chrysosporium*, the *lip* and *mnp* genes are present as gene families [6]. Pairwise comparisons among members of each family reach up to 98.9% identity [30], and it seems likely that this multiplicity arose as a result gene duplication events. The relatively low similarity of NoP with LiPs and MnPs (<50%, see below), and differences in gene structure suggests that incorporation of the *nop* gene into the genome was independent of the *lip* and *mnp* genes. On the other hand, the possibility that *nop* is an ancestor of *lip* and/or *mnp* genes cannot be ruled out.

3.2. The nop encoded sequence

Deduced from cDNA sequence, *nop* encodes a peroxidase of 315 amino acids, bearing a putative secretion signal [31] of 20 residues. Since most mature fungal peroxidases possess an average of 350 aa residues [4], attempts were made to predict an extra coding sequence in the C-terminal region. However, no additional domains could be identified after conceptual translation in the three reading frames. In addition, PCR reactions using primers extending further downstream failed to amplify any cDNAs.

To exclude sequencing errors and/or rearrangements during subcloning, the alternative allele and its corresponding cDNA were cloned and sequenced from the dikaryotic strain BKM-F-1767 (GeneBank accession numbers AY727766 and AY727767, respectively). Also, a cDNA was obtained from the strain ME446 (*nop*-m, AY727768). All these sequences, confirmed that *nop* encodes for a putative peroxidase that is shorter than all known Class II peroxidases.

Cladistic analysis was conducted including all non-redundant fungal peroxidases and a Class I peroxidase. As illustrated in Fig. 2, NoP groups apart from the MnPs and LiPs from *P. chrysosporium*, appearing more closely related to peroxidases from *C. cinereus* and *C. anamorph*.

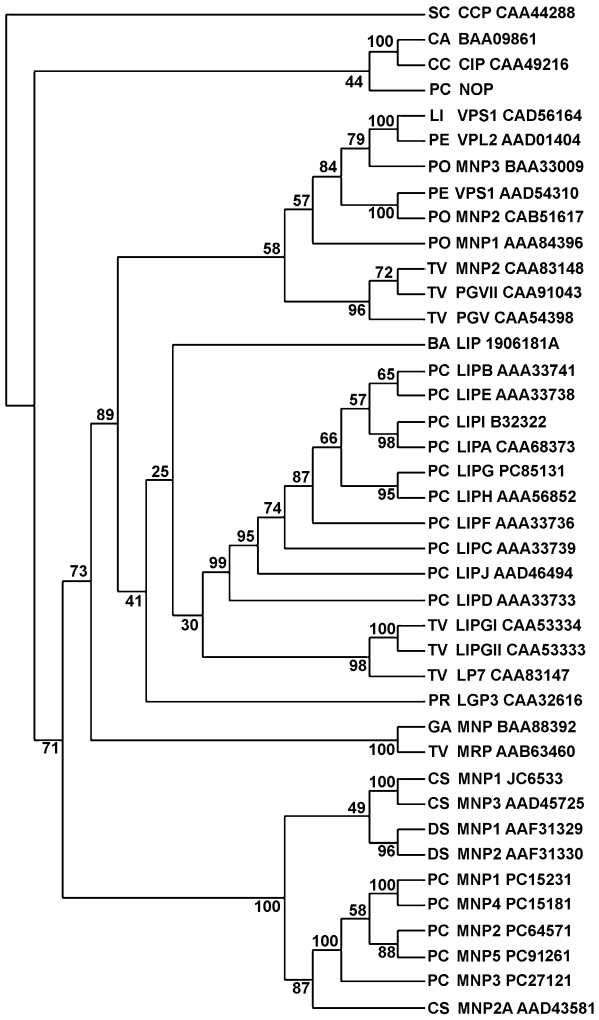

Fig. 2. Cladistic analysis of amino acid sequences of 38 different fungal peroxidases, a cytochrome *c* Class I peroxidase from *Saccharomyces cerevisiae* (SC CCP) and the NoP peroxidase (PC NOP). Cladogram from UPGMA. Abbreviations used for fungal species: CA—*Coprinus anamorph*; CC—*Coprinus cinereus*; PC—*Phanerochaete chrysosporium*; LI—*Lepista irina*; PE—*Pleurotus eryngii*; PO—*Pleurotus ostreatus*; TV—*Trametes versicolor*; BA—*Bjerkandera adusta*; PR—*Phlebia radiata*; GA—*Ganoderma applanatum*; CS—*Ceriporiopsis subvermispora* and DS—*Dichomitus squalens.* Numbers or letters added to the abbreviated name of each enzyme correspond to isoform variants. The last characters are database accession numbers.

Multiple alignment showed that NoP possesses overall identities in the range of 40–47% with most fungal peroxidases. Identity with LiPs and MnPs from *P. chrysosporium* falls below 43.8% (LiPJ) and 45.1% (MnP1), respectively.

3.3. Overall model structure and validation

The structure of NoP resembles that of Class II peroxidases (Fig. 3), although some structural differences were found that are characteristic of Class I or III family members. The NoP model resulted in a globular protein formed by eleven α-helices and four short β-sheets, with two domains defining a central cavity harboring the heme group. About 81.3% of residues were plotted in the most favored regions (A, B, L) of the Ramachandran plot. Forty-four residues (17.5%) fell in additional allowed regions and three residues (1.2%) were found to be in generously allowed regions. None of the residues was found in a disallowed region. Additional model validation using the Verify-3D program gave an overall self-compatibility score

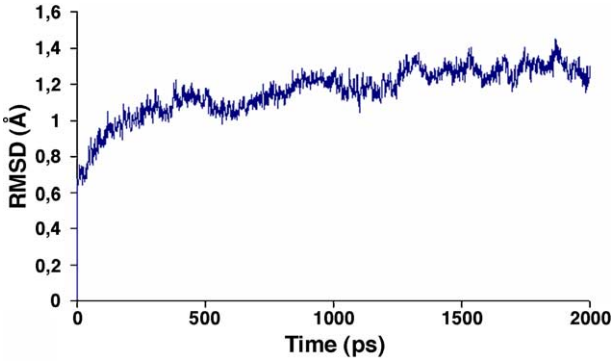

Fig. 4. C-alpha root-mean-square deviation (RMSD) computed against the NoP initial structure along 2 ns full atom MD simulation.

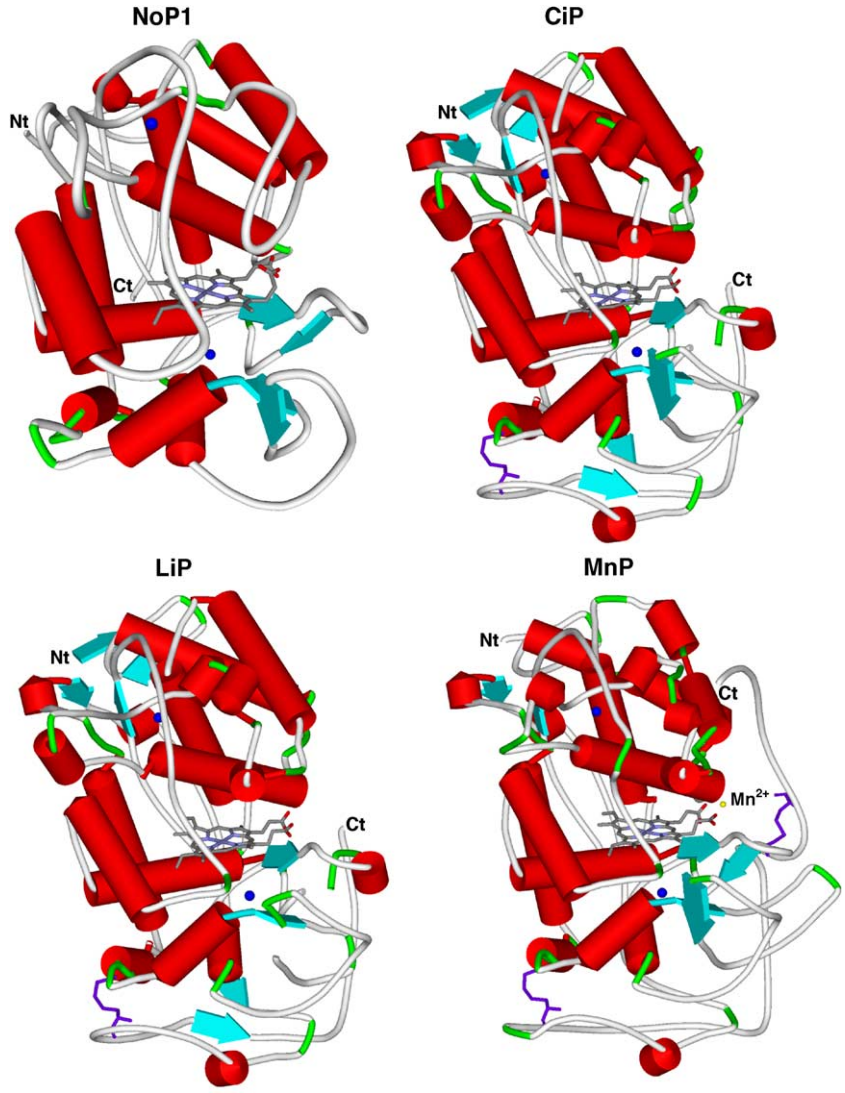

Fig. 3. Schematic representations of NoP (comparative model), CiP (PDB id: 1LYK), LiP2 (PDB id: 1LGA) and MnP1 (PDB id: 1MNP). Purple sticks in CiP, LiP and MnP represent disulfide bridges that are absent in NoP. Structural Ca^{2+} ions are represented in dark blue.

of 126.02 for an expected value of 134.22. Similar values were obtained by analysis of the templates used for modeling.

Considering the short length of the NoP mature protein and the presence of three instead of the expected four disulfide bonds (see below), a MD simulation was performed over the model to probe the stability of the structure. The overall conformational change of the trajectories was evaluated by the root-mean-square deviation (RMSD). The time-dependent change of backbone atoms RMSD from the initial structure was about 1.5 Å or lower (Fig. 4), indicating that the local structure of each domain was mostly conserved during the simulation.

3.4. Structural features of NoP

NoP lacks the C-terminal extension (about 60 residues) located in the outer layer of Class II and Class III peroxidases (Fig. 3). This domain does not bear any catalytic residue and, as assessed by MD, its absence does not affect the overall stability of the protein.

a) Disulfide bonds: crystallographic [32–34] and experimental [35] data have shown that LiPs and CiP possess four disulfide bonds, whereas MnPs have five of these linkages. The position of the eight Cys involved in the formation of the first four disulfide bonds is highly conserved in all fungal peroxidases (MnPs, CiP and LiPs). Four of these residues are located in the first 42 residues from the N-terminal region of the proteins. NoP presents six (1, 2, 3, 4, 5 and 7) of the eight Cys described in Class II peroxidases. The sixth Cys has been replaced by a Pro, whereas the eighth Cys would have been expected to be located in the C-terminal region absent in NoP (see Fig. 3).

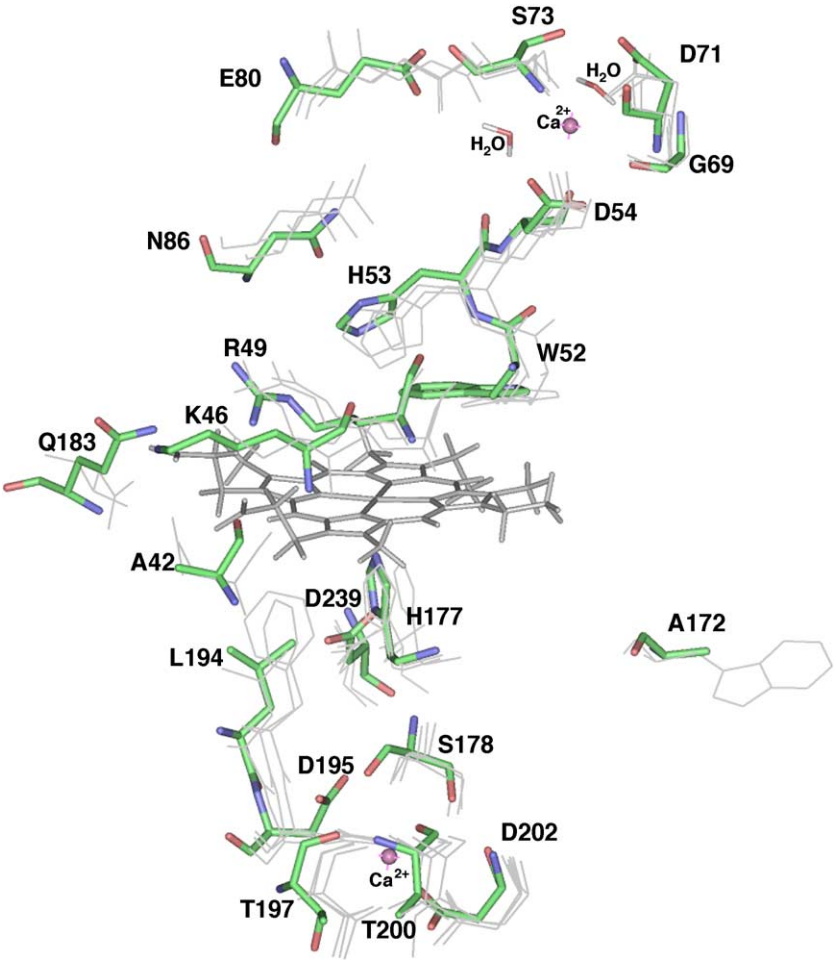

Fig. 5. Superimposition of amino acids side chains of NoP (colored residues), CiP, LiP and MnP (grey lines). The following residues are shown (NoP/Cip/Lip/Mnp): R49/R51/R43/R42, W52/F54/F46/F45, H53/H55/H47/H46, E80/E86/E78/E74, N86/N92/N84/N80, H177/H183/H176/H173, L194/L200/F193/F190 and D239/D245/D238/D242 in the distal and proximal heme pocket sides; D54/D56/D48/D47, G69/G74/G66/G62, D71/D76/D68/D64 and S73/S78/S70/S66 in the distal calcium binding site, where two water molecules were added to achieve the correct coordination geometry; S178/S184/S177/S174, D195/D201/D194/D191, T197/T203/T196/T193, T200/V206/I199/T196 and D202/D208/D201/D198 in the proximal calcium binding site. Also shown are the superimposed residues of NoP and MnP around the manganese binding site of the latter (NoP/MnP): A42/E36, K46/E40, Q183/D182 and the NoP A172 superimposed with the long-range aromatic substrate oxidation LiP W171.

b) Heme pocket residues: NoP presents all the residues in both sides of the heme group that have been shown to be required for activity [4,36,37]. The iron proximal side contains His177, Asp239 and Leu194. In Class II peroxidases, the latter position is normally filled with Phe (proximal Phe), with the exception of CiP and ARP, which also bear Leu [3,35] (Fig. 5). In turn, the conserved residues at the distal side include Arg49, His53, Asn86, Glu80 and Trp52. The identity of this last residue was unexpected, since all Class II peroxidases contain Phe (distal Phe) instead (Fig. 5). Class I peroxidases such as cytochrome *c* and ascorbate peroxidases also possess Trp instead of Phe in this position [38].

c) Metal binding sites: NoP lacks the residues required to bind Mn^{2+} that are present in MnPs and VPs. At the equivalent positions (Glu35, Glu39 and Asp179 in MnP1 from *P. chrysosporium* [34]), it possesses residues with either positive or neutral side chains that would produce a considerable electrostatic repulsion towards the Mn^{2+} ion. However, NoP conserves the residues involved in the coordination of two structural Ca^{2+} ions [39]. The distal Ca^{2+} is coordinated with five ligands from the main and side chains of residues Asp54, Gly69, Asp71 and Ser73, in a pentagonal bipyramidal geometry [40]. Two water molecules were added to achieve the correct geometry. The ligands of the proximal Ca^{2+} are eight atoms from residues Ser178, Asp195, Thr197, Thr200 and Asp202, which are distributed around the metal with an octahedral geometry.

d) Sites for substrate oxidation: the oxidation of small aromatic substrates takes place at the vicinity of the heme cavity. In LiP, the residues interacting with the substrate are His82 and Gln222 located at the entry of the heme access channel [32]. These residues also appear conserved in VPS1 but not in VPL from *Pleurotus eryngii* [41]. Corresponding positions in NoP are occupied by Pro84 and Lys223. On the other hand, a hydrophobic region in CiP composed of Arg52, His54 and Pro156 located deep inside the heme pocket, together with Ala92, Leu192 and Phe230 placed at its entrance, could form favorable interactions with aromatic substrates [42,43]. A similar topology with residue conservation was found in NoP, with Arg49, His53 and Pro143 found at the bottom of the pocket and residues Ala85, Val185 and His222 placed at its entrance.

In addition, three long-range electron transfer pathways have been suggested in LiP [4]. One of them involves Pro83, Asn84 and His82 located at the edge of the heme channel. Corresponding residues in NoP are Ala85, Asn86 and Pro84. A second pathway also initiates in the superficial His239 and continues through Asp238 and His176. In NoP the last two residues are conserved, namely Asp239 and proximal His177, but His239 is replaced by Gly240. The third pathway in LiP starts with Trp171 and proceeds through Met172 or Leu172. Trp171 is conserved in all LiPs and it is absent in MnPs and CiP. In NoP, the equivalent position is occupied by Ala172. Due to the lack of conservation in the residues involved in the proposed pathways, predictions about long-range electron transfer in NoP are difficult to assess.

Acknowledgements

This work was financed by the Millenium Institute for Fundamental and Applied Biology, by grant 1030495 from FONDECYT and the U.S. Department of Energy grant DE-FG02-87ER13712.

References

[1] J. Everse, The structure of heme proteins compounds I and II: some misconceptions, Free Radic. Biol. Med. 24 (1998) 1338–1346.
[2] H.B. Dunford, Heme Peroxidases, Wiley-VCH, New York, 1999.
[3] K.G. Welinder, Superfamily of plant, fungal and bacterial peroxidases, Curr. Opin. Struct. Biol. 2 (1992) 388–393.
[4] A.T. Martínez, Molecular biology and structure-function of lignin-degrading heme peroxidases, Enzyme Microb. Technol. 30 (2002) 425–444.
[5] T.K. Kirk, R.L. Farrell, Enzymatic ''combustion'': the microbial degradation of lignin, Annu. Rev. Microbiol. 41 (1987) 465–505.
[6] D. Martinez, L.F. Larrondo, N. Putnam, M.D. Sollewijn-Gelpke, K. Huang, J. Chapman, K.G. Helfenbein, P. Ramaiya, J.C. Detter, F. Larimer, P.M. Coutinho, B. Henrissat, R. Berka, D. Cullen, D. Rokhsar, Genome sequence of the lignocellulose degrading fungus *Phanerochaete chrysosporium* strain RP78, Nat. Biotechnol. 22 (2004) 695–700.
[7] L.F. Larrondo, L. Salas, F. Melo, R. Vicuña, D. Cullen, A novel extracellular multicopper oxidase with ferroxidase activity in *Phanerochaete chrysosporium*, Appl. Environ. Microbiol. 69 (2003) 6257–6263.
[8] L.F. Larrondo, B. González, D. Cullen, R. Vicuña, Characterization of a multicopper oxidase gene cluster in *Phanerochaete chrysosporium* and evidence of altered splicing of the mco transcripts, Microbiology 150 (2004) 2775–2783.
[9] J. Dittmer, N. Patel, S. Dhawale, S. Dhawale, Production of multiple laccase forms by *Phanerochaete chrysosporium* grown under nutrient sufficiency, FEMS Microbiol. Lett. 149 (1997) 65–70.
[10] C.S. Rodriguez, R. Santro, C. Cameselle, A. Sanroman, Laccase production in semi-solid cultures of *Phanerochaete chrysosporium*, Biotechnol. Lett. 19 (1997) 995–998.
[11] H. Podgornik, M. Stegu, E. Zibert, A. Perdih, Laccase production by *Phanerochaete chrysosporium*—an artefact caused by Mn(III)? Lett. Appl. Microbiol. 32 (2001) 407–411.
[12] P. Stewart, J. Gaskell, D. Cullen, A homokaryotic derivative of a *Phanerochaete chrysosporium* strain and its use in genomic analysis of repetitive elements, Appl. Environ. Microbiol. 66 (2000) 1629–1633.
[13] A.V. Wymelenberg, S. Denman, D. Dietrich, J. Bassett, X. Yu, R. Atalla, P. Predki, U. Rudsander, T.T. Teeri, D. Cullen, Transcript analysis of genes encoding a family 61 endoglucanase and a putative membrane-anchored family 9 glycosyl hydrolase from *Phanerochaete chrysosporium*, Appl. Environ. Microbiol. 68 (2002) 5765–5768.
[14] A. Manubens, M. Avila, P. Canessa, R. Vicuña, Differential regulation of genes encoding manganese peroxidase (MnP) in the basidiomycete *Ceriporiopsis subvermispora*, Curr. Genet. 43 (2003) 433–438.

[15] F.M. Ausubel, R. Brent, R.E. Kingston, D.D. Moore, J.G. Seidman, J.A. Smith, K. Struhl, Short Protocols in Molecular Biology, 2nd ed., Greene Publishing Associates, New York, 1992.
[16] S.F. Altschul, W. Gish, W. Miller, E.W. Myers, D.J. Lipman, Basic local alignment search tool, J. Mol. Biol. 215 (1990) 403–410.
[17] J.D. Thompson, T.J. Gibson, F. Plewniak, F. Jeanmougin, D.G. Higgins, The ClustalX windows interface: flexible strategies for multiple sequence alignment aided by quality analysis tools, Nucleic Acids Res. 24 (1997) 4876–4882.
[18] D.F. Feng, R.F. Doolittle, Progressive alignment of amino acid sequences and construction of phylogenetic trees from them, Methods Enzymol. 266 (1996) 368–382.
[19] S. Kumar, K. Tamura, M. Nei, MEGA3: integrated software for molecular evolutionary genetics analysis and sequence alignment, Brief. Bioinform. 5 (2004) 150–163.
[20] M. Nei, S. Kumar, Molecular Evolution and Phylogenetics, Oxford University Press, New York, 2000.
[21] A. Sali, T.L. Blundell, Comparative protein modelling by satisfaction of spatial restraints, J. Mol. Biol. 234 (1993) 779–815.
[22] R.A. Laskowski, M.W. MacArthur, D.S. Moss, J.M. Thornton, PROCHECK: a program to check the stereochemical quality of protein structures, J. Appl. Crystallogr. 26 (1993) 283–291.
[23] J.U. Bowie, R. Luthy, D. Eisenberg, A method to identify protein sequences that fold into a known three-dimensional structure, Science 253 (1991) 164–170.
[24] R. Luthy, J.U. Bowie, D. Eisenberg, Assessment of protein models with three-dimensional profiles, Nature 356 (1992) 83–85.
[25] K. Houborg, P. Harris, J.F.W. Petersen, P. Rowland, J.C. Poulsen, P. Schneider, J. Vind, S. Larsen, Impact of the physical and chemical environment on the molecular structure of *Coprinus cinereus* peroxidase, Acta Crystallogr., Sect. D 59 (2003) 989–996.
[26] K. Tsukamoto, H. Itakura, K. Sato, K. Fukuyama, S. Miura, S. Takahashi, H. Ikezawa, T. Hosoya, Binding of salicylhydroxamic acid and several aromatic donor molecules to *Arthromyces ramosus* peroxidase, investigated by X-ray crystallography, optical difference spectroscopy. NMR relaxation, molecular dynamics, and kinetics, Biochemistry 38 (1999) 12558–12568.
[27] W. Yang, H.W. Lee, H. Hellinga, J. Yan, Structural analysis, identification, and design of calcium-binding sites in proteins, Prot. Struct. Funct. Genet. 47 (2002) 344–356.
[28] J.F.W. Petersen, A. Kadziola, S. Larsen, Three-dimensional structure of a recombinant peroxidase from *Coprinus cinereus* at 2.6 Å resolution, FEBS Lett. 339 (1994) 291–296.
[29] H. Sawaihatanaka, T. Ashikari, Y. Tanaka, Y. Asada, T. Nakayama, H. Minakata, N. Kunishima, K. Fukuyama, H. Yamada, Y. Shibano, T. Amachi, Cloning, sequencing and heterologous expression of a gene coding for *Artromyces ramosus* peroxidase, Biosci. Biotechnol. Biochem. 59 (1995) 1221–1228.
[30] D. Cullen, Recent advances on the molecular genetics of ligninolytic fungi, J. Biotechnol. 53 (1997) 273–289.
[31] H. Nielsen, J. Engelbrecht, S. Brunak, G. von Heijne, Identification of prokaryotic and eukaryotic signal peptides and prediction of their cleavage sites, Protein Eng. 10 (1997) 1–6.
[32] T.L Poulos, S.L. Edwards, H. Wariishi, M.H. Gold, Crystallographic refinement of lignin peroxidase at 2 A, J. Biol. Chem. 268 (1993) 4429–4440.
[33] K. Houborg, P. Harris, J.C. Poulsen, P. Schneider, A. Svendsen, S. Larsen, The structure of a mutant enzyme of *Coprinus cinereus* peroxidase provides an understanding of its increased thermostability, Acta Crystallogr., Sect. D 59 (2003) 997–1003.
[34] M. Sundaramoorthy, K. Kishi, M.H. Gold, T.L. Poulos, Crystal structures of substrate binding site mutants of manganese peroxidase, J. Biol. Chem. 272 (1997) 11780–17574.
[35] P. Limongi, M. Kjalke, J. Vind, J.W. Tams, T. Johansson, K.G. Wellinder, Disulfide bonds and glycosylation in fungal peroxidases, Eur. J. Biochem. 227 (1995) 270–276.
[36] L. Banci, Structural properties of peroxidases, J. Biotechnol. 53 (1997) 253–263.
[37] A. Conesa, P.J. Punt, C.A.M.J.J. van den Hondel, Fungal peroxidases: molecular aspects and applications, J. Biotechnol. 93 (2002) 143–158.
[38] M. Zámocký, Phylogenetic relationships in class I of the superfamily of bacterial, fungal and plant peroxidases, Eur. J. Biochem. 271 (2004) 3297–3309.
[39] B.D. Howes, A. Feis, L. Raimondi, C. Indiani, G. Smulevich, The critical role of the proximal calcium ion in the structural properties of horseradish peroxidase, J. Biol. Chem. 276 (2001) 40704–40711.
[40] W. Yang, H.W. Lee, H. Hellinga, J.J. Yang, Structural analysis, identification, and design of calcium-binding sites in proteins, Proteins 47 (2002) 344–356.
[41] S. Camarero, S. Sarkar, F.J. Ruiz-Dueñas, M.J. Martínez, A.T. Martínez, Description of a versatile peroxidase involved in natural degradation of lignin that has both Mn-peroxidase and lignin-peroxidase substrate binding sites, J. Biol. Chem. 274 (1999) 10324–10330.
[42] H. Itakura, Y. Oda, K. Fukuyama, Binding mode of benzhydroxamic acid to *Arthromyces ramosus* peroxidase shown by X-ray crystallographic analysis of the complex at 1.6 Å resolution, FEBS Lett. 412 (1997) 107–110.
[43] K. Tsukamoto, H. Itakura, K. Sato, K. Fukuyama, S. Miura, S. Takahashi, H. Ikezawa, T. Hosoya, Binding of salicylhydroxamic acid and several aromatic donor molecules to *Arthromyces ramosus* peroxidase, Investigated by X-ray crystallography, optical difference spectroscopy, NMR relaxation, molecular dynamics, and kinetics, Biochemistry 38 (1999) 12558–12568.